



# Improved Magnetic Sensor for Oil and Natural Gas Well Logging

*DESIGN DOCUMENT*



## TEAM MEMBERS

MARION OKOTH (TEAM LEAD)

ELIZABETH CLARKIN (WEBMASTER)

MATTHEW MULLOY (COMMUNICATIONS)

## ADVISORS

DR. RAVI HADIMANI

NEELAM PRAHBU

DEC15-17

## Table of Contents

Table of figures .....	2
Introduction.....	4
Executive summary.....	4
Motivation .....	4
Deliverables .....	4
Specifications.....	5
System Level Design.....	6
Functional requirements:.....	6
Non-Functional requirements:.....	6
Design Description .....	7
Interface specifications.....	7
Software Specifications.....	7
Parts List .....	8
Magnetic Core Sample Preparation .....	8
Simulations and Modeling .....	9
Implementation Issues and Challenges.....	12
Testing, Procedures and Specifications.....	13
Anomalous resonant frequencies .....	24
Conclusion .....	27
References .....	28

## Table of figures

Figure 1. MATLAB code for FFT. ....	7
Figure 2. Schematic of Sample preparation method. ....	9
Figure 3. Seven Neodymium Boron magnets stacked. ....	10
Figure 4. Cylindrical material core radially ....	10
Figure 5. Cylindrical material core laterally in geometric center of stacked magnets. ....	11
Figure 6. Cylindrical Giron shielding surrounding magnets and shielding. ....	11
Figure 7. Hysteresis graph measurements of current samples. ....	13
Figure 8. Zoom in figure 6 showing coercivity. ....	14
Figure 9. Measurement setup. ....	15
Figure 10. Filtered signal and filter from Duplexer. ....	16
Figure 11. Decaying pulse signal. ....	16
Figure 12. Sample Mu55-2 0.9 MHz. ....	17
Figure 13. Sample Mu55-2 0.396 MHz. ....	17
Figure 14. Sample Mu55-2 0.424 MHz. ....	17
Figure 15. Assembled new sample holder with the increased magnetic field without top cover. ....	18
Figure 16. Center frequency 156.9 kHz. ....	18
Figure 17. Center frequency 424 kHz. ....	19
Figure 18. Center frequency 494 kHz. ....	19
Figure 19. Center frequency 128.2 kHz. ....	19
Figure 20. Center frequency 240 kHz. ....	19
Figure 21. Center frequency 404 kHz. ....	20
Figure 22. Center frequency 476.4 kHz. ....	20
Figure 23. Center frequency 479.8 kHz. ....	20
Figure 24. Center frequency 495 kHz. ....	20
Figure 25. Center frequency 507.8 kHz. ....	20
Figure 26. Center frequency 682 kHz. ....	21
Figure 27. Center frequency 911.2 kHz. ....	21
Figure 28. Center frequency 951.6 kHz. ....	21
Figure 29. Center frequency 156.9 kHz. ....	21
Figure 30. Center frequency is 212 kHz. ....	22
Figure 31. Center frequency 214 kHz. ....	22

Figure 32. Center frequency 424.2 kHz. ....	22
Figure 33. Center frequency 457 kHz. ....	22
Figure 34. Center frequency 494.8 kHz. ....	23
Figure 35. Center frequency 678.5 kHz. ....	23
Figure 36. Center frequency 752 kHz. ....	23
Figure 37. Comparison of MU70, MU55 and Ferrite epoxy peaks. ....	24
Figure 38. Anomalous peak center frequency 229 kHz for MU70 (increased magnetic field). ....	24
Figure 39. Anomalous peak center frequency 1.135 kHz MU70 (increased magnetic field). ....	25
Figure 40. Circuit simulation schematic. ....	25
Figure 41. Transient analysis result center frequency 156.9 kHz. ....	26
Figure 42. Frequency spectrum center frequency 156.9 kHz. ....	26
Figure 43. Zoom in of figure 42. ....	27

## Introduction

### Executive summary

The purpose of this project is to produce a low field magnetic sensor that has a high signal to noise ratio and that can also eliminate unwanted resonances brought about by losses in the measurement system. The sensor will be part of a Nuclear Magnetic Resonance setup used to characterize underground formations.

### Motivation

Nuclear Magnetic Resonance (NMR) spectroscopy is used in multiple different industries such as medical and chemical. A key application of this technology is used in the oil and gas industry where, it is used to acquire information about underground rock formations. This is done by embedding a Low Field NMR sensor into a drill tool used for down-hole drilling. The key component of the magnetic sensor, an inductive RF antenna with a soft core which surrounds the magnet. When a permanent static magnetic field is induced in an underground formation, it magnetizes the materials around it. If a perturbing RF field is introduced orthogonally to the static field it causes a spin flip in the magnetized particles. When the RF pulse is turned off, the spin states return to their previous state releasing an RF signal at the resonant frequency of the spin flip. The purpose of the magnetic core sensor is to amplify the incoming RF signal from the formation. From the frequency spectrum of the RF signal, the desired underground formation such as Oil and Natural gas pockets can found. Our client has such a sensor but they produce additional frequencies to the resonant spin flip frequency. This creates an error in the measurements by not returning accurate readings. They believe that these inaccuracies are due to the resonance frequencies of the material in the core of their sensor which are being induced within the material. Therefore, they have asked Iowa State University to help them find the source of these resonance frequencies (or at least calibrate them), and/or produce a better core material. Our senior design group is assisting by improving the testing setup with a uniform magnetic field, making and analyzing the measurements themselves, and writing a code to aid in the data analysis of these measurements.

### Deliverables

#### *Fall 2015*

At the end of this project we will provide the client with a first improvement in the constant magnetic field generation unit for the magnetic sensor measurement setup. The magnetic sensor will have a suitable magnetic core material which reduces/identify unwanted resonances. There will also be data from the characterization of the materials based on

magnetic measurements and ringing measurements available for the client. The client will also be provided with a GUI that processes all of the measurements for multiple materials, a stable magnetic field produced via an arrangement of permanent magnets and shielding, and a measurements of the materials provided by our client.

### Specifications

The magnetic sensor should have a high signal to noise ratio and should reduce the high ringing in the sample among other losses. The measurement setup has to be redesigned to include a uniform permanent magnetic field of around 400 Gauss. The sensor in question will be utilized for logging down-hole oil and gas reservoirs by the client so it has to be accurately calibrated.

## System Level Design

### Functional requirements:

- Ferrite epoxy soft magnetic core samples.
- Rod-like geometry.
- Reduce unwanted acoustics.
- Low Hysteresis losses.
- Uniform magnetic field of 400 Gauss encompassing the entire length of the ferrite core using neodymium boron (NIB) permanent magnets
- Each material we be looked at multiple frequencies. For each of the frequencies a csv file will be output containing the voltage and corresponding times.
- For each file, the entries will be Fourier transformed and the frequency of its max amplitude and its half width maximum (hwm) will be found.
- The results found in each file will be saved to a single file containing the max frequency and hwm for all files in the folder.
- This new file will be used to generate a chart comparing the hwm with the frequency of the test pulse.
- This process will be repeated for all material folders inside of a larger test folder

### Non-Functional requirements:

- Must be one of the materials currently being explored by the client.
- The magnetic core samples have to be prepared using the equipment available at Ames Lab or the Microelectronic Research Center (MRC).

## Design Description

### Interface specifications

The device will consist of a magnetic sensor with soft magnetic core that is surrounded by a static magnetic field provided by either a permanent magnet. The antenna is further attached to instruments such as a spectrometer, transmitter and receiver attached to it. The magnetic core is made of a soft magnetic material epoxy. To aid in the data analysis, a Graphical User Interface (GUI) will be created to allow the user process the data en masse. This program will require the user to select a folder. Once the folder has been selected the user will hit go and for each material folder in the original folder a secondary GUI will be opened. This secondary GUI will contain two charts. The first will display the amplitude against the frequency for the max of each test on the material. The second chart will display the half-width maximum against the frequency. These values will also be stored in text documents to aid further processing that the client might wish to perform.

### Software Specifications

The code will be written in MATLAB. The signals will be transformed and aligned using the Fast Fourier Transform (*fft*) function. The frequency of the max amplitude will be found using a “for loop”, that compares the each amplitude with the previous maximum, as seen below.

```
max_amp=1;
num_max=0
for i=1:le
    if (spect (i) == spect (max_amp))
        num_max=num_max+1
    end

    if (spect (i) >= spect (max_amp))
        max_amp=i
    end
end
```

Figure 1. MATLAB code for FFT.



### Parts List

Item	Qty.	Ref.	Cost	Part Desc.	Supplier
1	1	T1	\$ 16.60	0.5" diameter plastic tubes	Tap Plastics
2	1	P1	NA	Manganese Oxide	Client
3	1	P2	\$ 34.74	Zinc Oxide	Chemistry Lab
4	1	P3	NA	Iron Oxide	Client
5	1	P4	\$ 89.00	Nickel Oxide	Fisher Scientific
6	7	P4	\$ 29.99	NIB magnet	Magnets4less
7	3	P4	\$ 44.95	Giron (25.5 in x 12 in)	Less EMF

### Magnetic Core Sample Preparation

One of the sample will be prepared at Ames Lab facility in Wilhem hall. This preparation will consist of Ferric oxide, Manganese or Nickle oxide and Zinc oxide to produce  $Mn_{1-x}Zn_xFe_2O_4$  or  $Ni_{1-x}Zn_xFe_2O_4$  powders. The value of x will vary from 0.2 to 0.8. The ratio of sample powder to epoxy will vary from 20/80, 40/60, 60/40 and 80/20 respectively.

Initially the sample powders were batch mixed in a glass jar to improve homogenization. Ball milling was the next stage to create intimate contact between the particles. The ball mill used different sizes of lead balls to vary the particle size. Compaction of the sample with a hydraulic press was then done after the ball milling stage before every calcination step. Once the sample was compacted, it was calcined at 1050-1100 °C to create a solid state reaction. The sample will underwent two more ball milling stages and one more calcination stage before it was ready to be mixed with epoxy. Sieving was done after the last ball milling stage to remove particles that were not properly milled. The schematic of the sample preparation process is shown in figure 2.

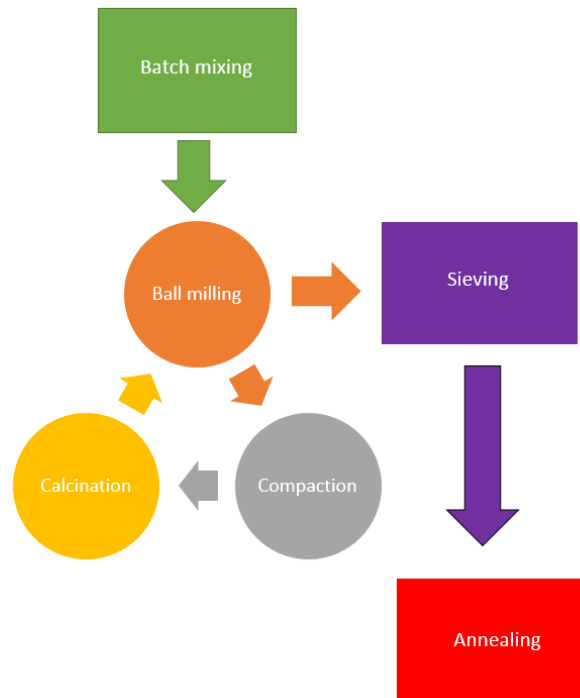


*Figure 2. Schematic of Sample preparation method.*

After the last ball milling stage, annealing may be introduced to produce a two-phase nanocrystalline and amorphous microstructure, with the crystalline grains being randomly distributed [1]. There are studies that have shown that annealing increases the permeability and reduces coercivity of soft magnetic ferrite powders [2]. The optimal annealing temperature will be chosen so that the microstructure is not completely crystalline to reduce perpendicular anisotropy in the sample. Annealing will also have to be done in vacuum or an inert surface to prevent oxidation. This method may be used in the future.

Currently, the client is using Ferrite Epoxy samples for testing. They will be made by batch mixing Ni-Zn Ferrite commercial powder or powders mixed by the client with epoxy.

### **Simulations and Modeling**

It has been decided through calculations and simulations that the obvious answer of creating a magnetic field using a solenoid will not produce the required result for this project. The magnetic field requirement of 400 Gauss is too small; the turn ratio density of the solenoid would be too low. This would allow magnetic flux leakage that would hamper the uniform magnetic field and create inconsistent asymmetry. Therefore, it has been decided to create the magnetic field using neodymium boron (NIB) permanent magnets.

The uniform static magnetic fields are being simulated in COMSOL. The cylindrical shape of the materials necessitated the cylindrical surrounding disk shape of the magnets. The magnetic flux from the Nib to the core material is a predictable constant. So the internal magnetic field of each core material is therefore variable based on that materials relative permeability. By surrounding the magnets and material with a shield (figure 6), the magnetic flux though the core can be limited and internal material flux variation can be reduced or removed.

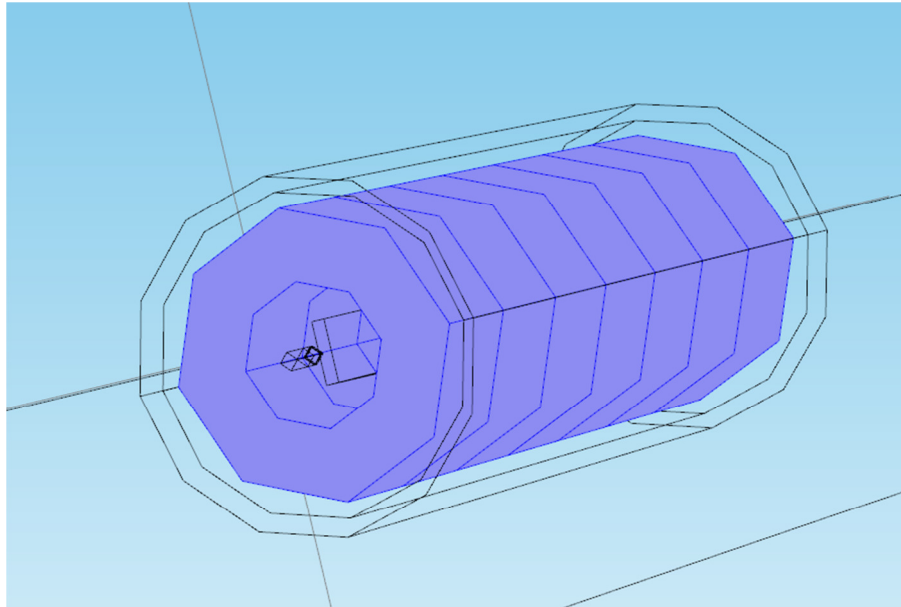


*Figure 3. Seven Neodymium Boron magnets stacked.*

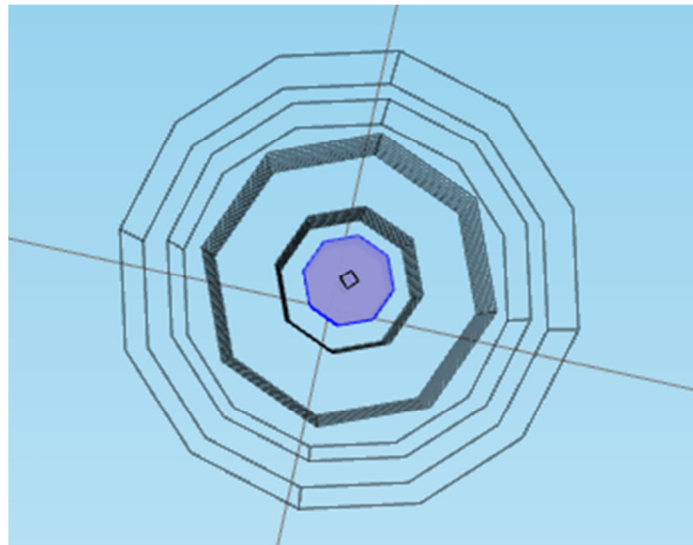


*Figure 4. Cylindrical material core radially  
(Hexagon shape due to user interface lag. Mesh simulation is cylindrical).*

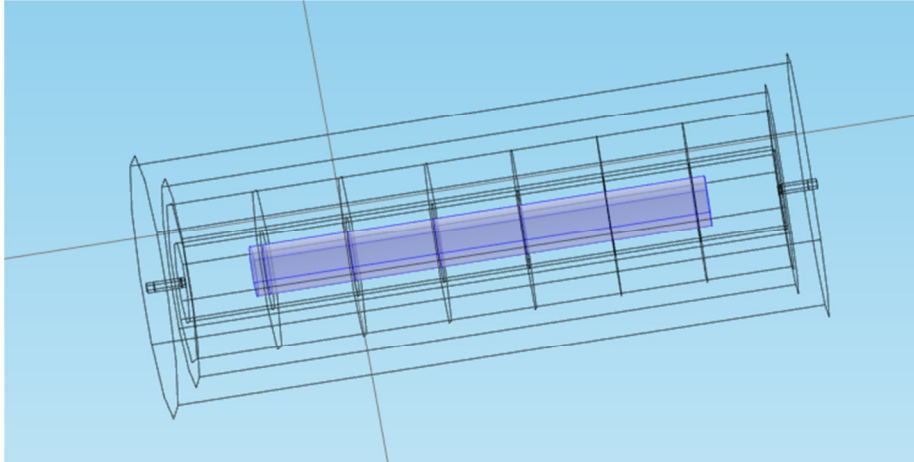


*Figure 5. Cylindrical material core laterally in geometric center of stacked magnets.*

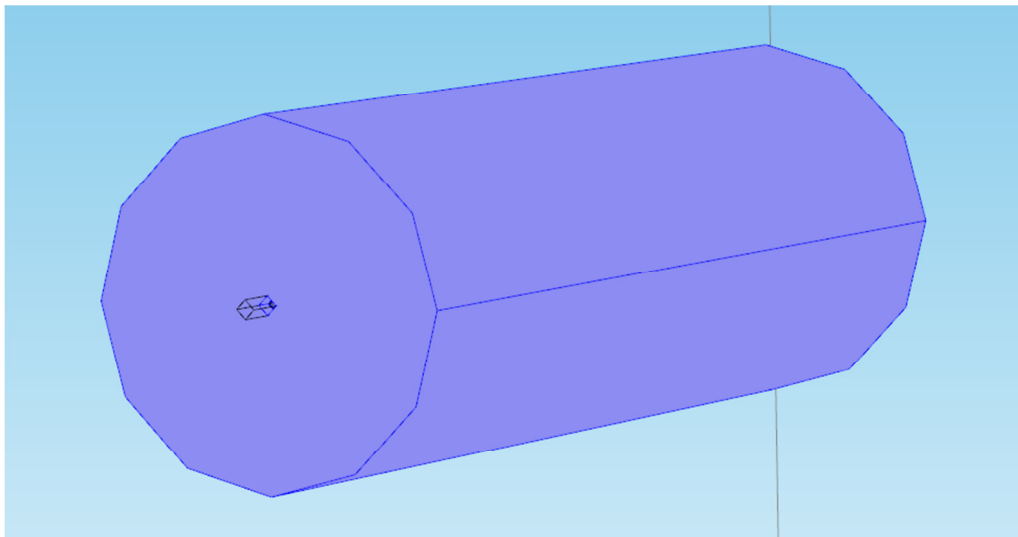


*Figure 6. Cylindrical Giron shielding surrounding magnets and shielding.*

Therefore, for each material presented, given that materials geometry and relative permeability, a uniform magnetic field through any material can be created. The variables to accomplish this are;

- the number of magnets stacked on each other, thereby increasing the magnetic field and increasing the distance from the material laterally to the edge of the permanent magnet laterally
- the distance from the permanent magnet design to the shielding lengthwise, allowing more flux to enter the core material but increasing the variation inside

- the distance from the magnet design to the shielding material radially, allowing for less saturation of the material and more flux to enter the core material
- the thickness of the shield, thicker shielding allowing for more flux saturation

Good simulation results have been obtained for each of the four materials currently under experimentation. Below is the linear characteristic for SA 70 though the core material lengthwise from the end. Notice the variation in the magnetic field from the maximum to the local minimum in the center. The simulation compares the core to air in the same geometry

### Implementation Issues and Challenges

For the magnetic core, the biggest issues will be getting the materials made in a timely manner. No one on our group was able to get an associateship with Ames Lab where the materials will be produced. This means we have to rely on Ames Lab staff or our graduate student advisor to make the samples for us.

Another challenge will be implementing the annealing process into the sample preparation to improve the soft magnetic properties. This process is time consuming due to slow cooling required. If the as prepared sample without annealing shows adequate soft magnetic properties the process may not be done.

Also, if the sample preparation methods we have chosen don't yield the results we want, it will be difficult for us to change the material since we are limited to the samples provided by the client group.

For the permanent magnet, the largest issue is the need for customization for each core material based of that material's relative permeability and geometry. The neodymium boron magnets can be reused for each material. But the Giron shielding will need to be customized. This increases both cost and time for creation of each shielding geometry. Also, a nonmagnetic polymer material to hold the geometry constant will need to be found and created.

There are two potential problems with software. The first is the implementation of the *fft* using the actual measured data. To address this, testing will be done using a simple sinusoidal function first. The second is communication between portions of the GUI and between the GUI and its subGUIs'. This is a very messy process that has a lot of detail. There are however many online resources which we are utilizing to aid in the process.

### Testing, Procedures and Specifications

The testing plan semester was to first characterize the material. Measurements on the samples were performed to find their coercivity using the Hysteresis graph. The machine used is the AMH-300 Hysteresis Graph measurement machine. Preliminary hysteresis graph measurements were performed with a solenoid providing the magnetic field. The solenoid had a B coil with 1000 turns. The results are shown in figures 9 and 10.

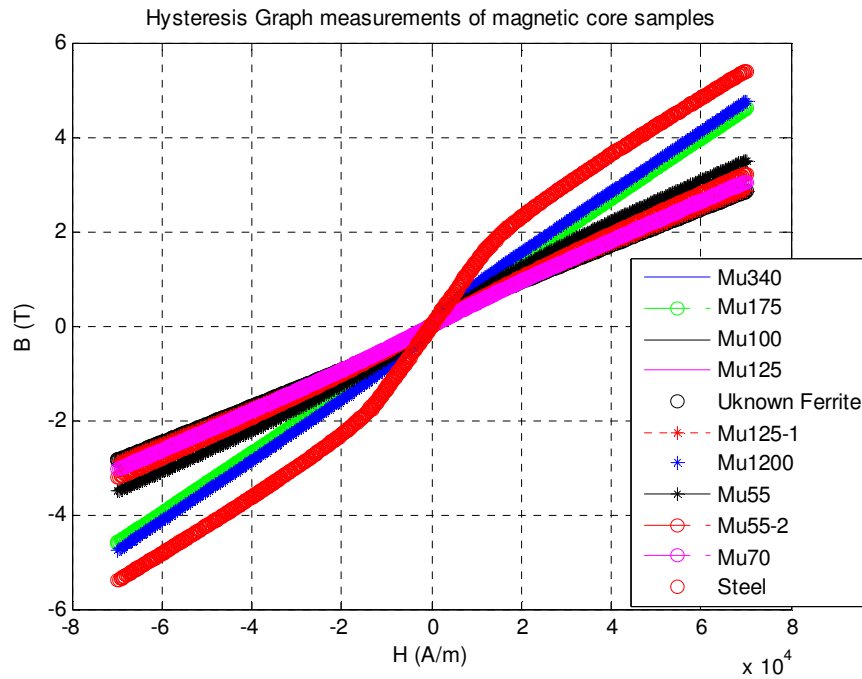


Figure 7. Hysteresis graph measurements of current samples.

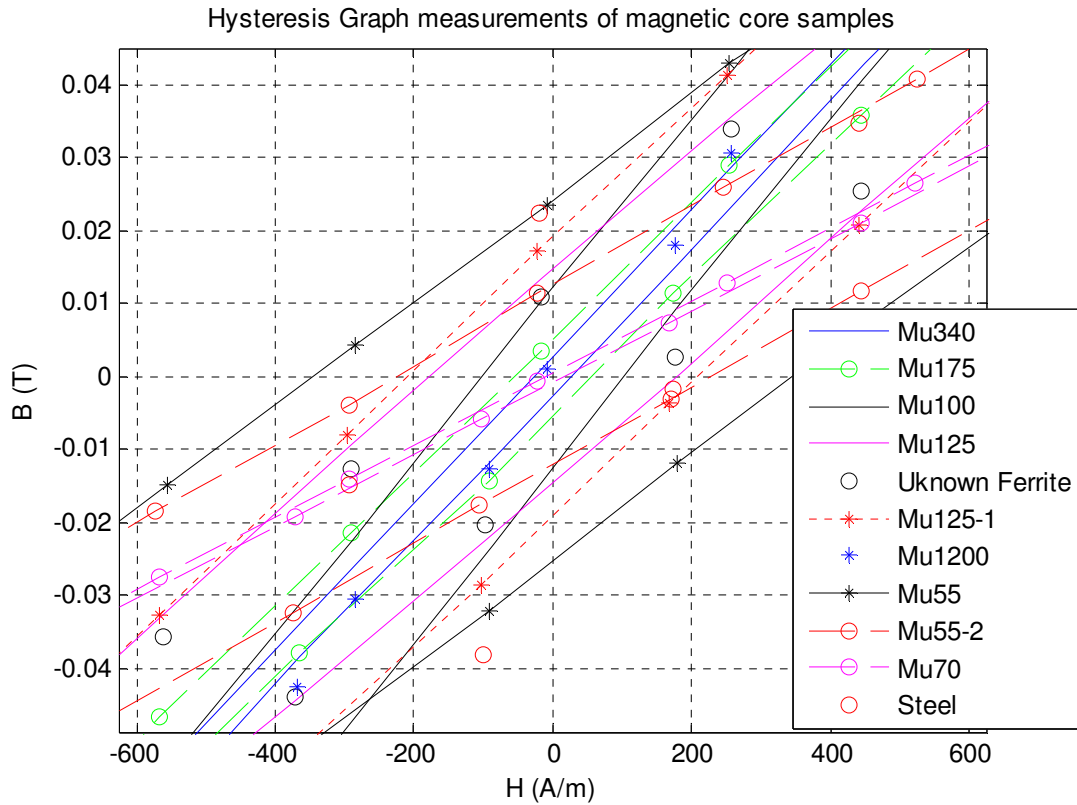


Figure 8. Zoom in figure 6 showing coercivity.

Coercivity of the samples was found by finding the value of the applied field  $H$  when  $B$  was 0. The coercivity measurements are shown in table 1.

Table 1: Coercivity measurements

Sample Number	$H_c$ (A/m)	$B_r$ (T)
Mu340	27.25	0.00275
Mu175	56.9	0.005265
Mu100	102.1	0.0122
Mu125	178.5	0.015
Unknown ferrite	143.885	0.0124
Mu125-1	208.84	0.0192
Mu1200	17.68	0.0199
Mu55	346.015	0.0243
Mu55-2	227.01	0.0127
Mu70	14.19	0.00069
Steel	185.4	0.0252

The magnetic material did not saturate as shown in figure 9. Therefore, the coercivity results shown in table 1 are not accurate. For future measurements the magnetic field will be provided by an Electromagnet which can be utilized to obtain higher magnetic fields.

The code will be tested on data that has already been processed. The results of the code will be compared with the existing results. First individual samples will be tested then batches of multiple frequencies for a single material will be processed. Finally we will test a file containing multiple materials.

The as prepared samples were tested using the measurement setup shown in figure 9.

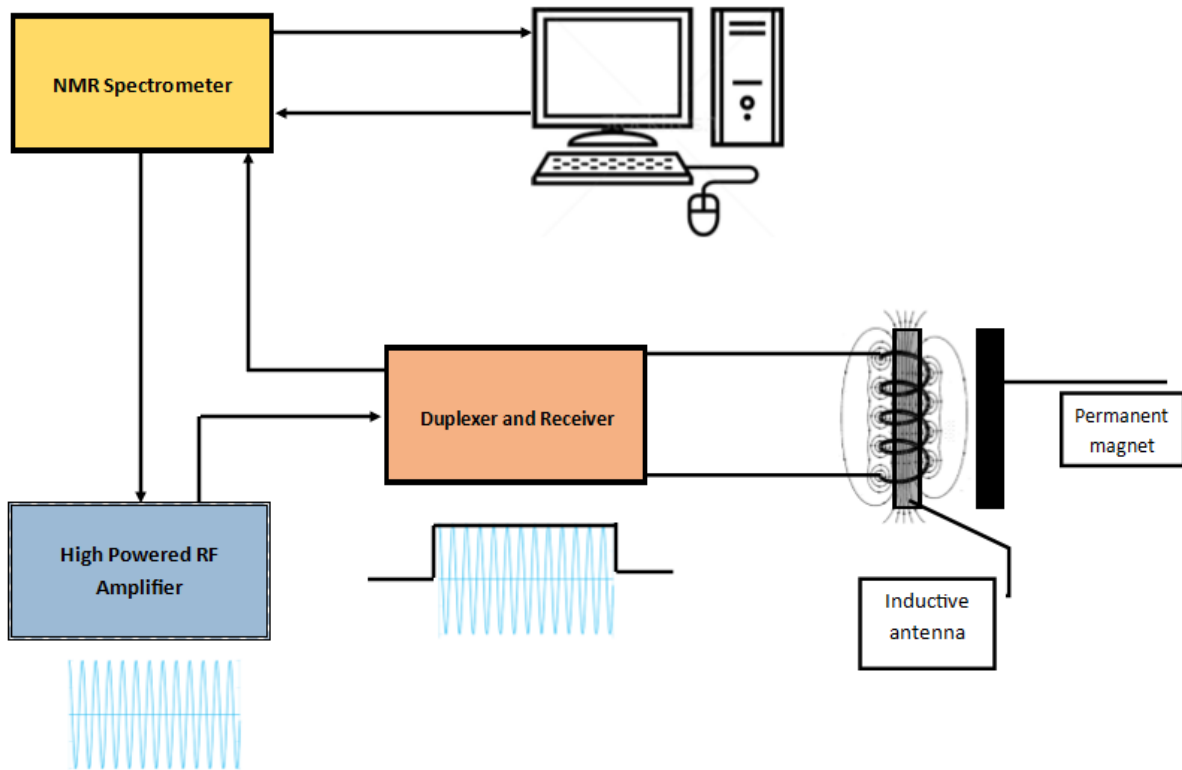


Figure 9. Measurement setup.

The measurement setup works as follows, the user defines a low power pulse sinusoid signal which is routed to the NMR spectrometer. The signal is sent to the high power RF amplifier which increase its power. The amplified signal is routed to a duplex which filters out all signals which are not of a particular frequency band before it routes it onto the inductive load. In our current measurements, the external field is provided by an N52 permanent magnet. The external field is not considered uniform for now.

The filtered pulsed sinusoid signal and the filter of the duplexer are shown in figure 10.



DEC15-17  
IMPROVED MAGNETIC SENSOR FOR OIL AND NATURAL GAS WELL LOGGING

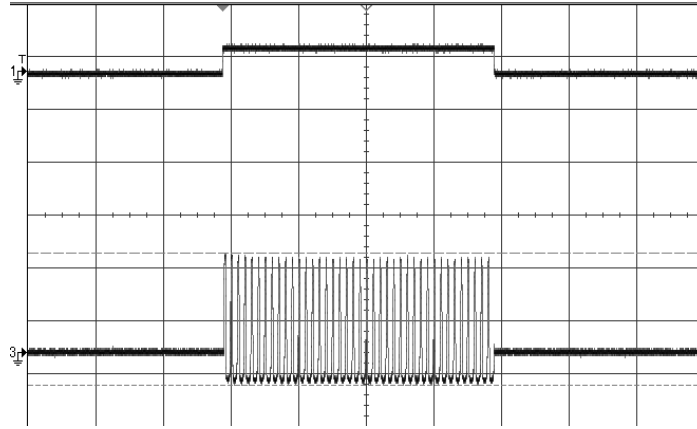


Figure 10. Filtered signal and filter from Duplexer.

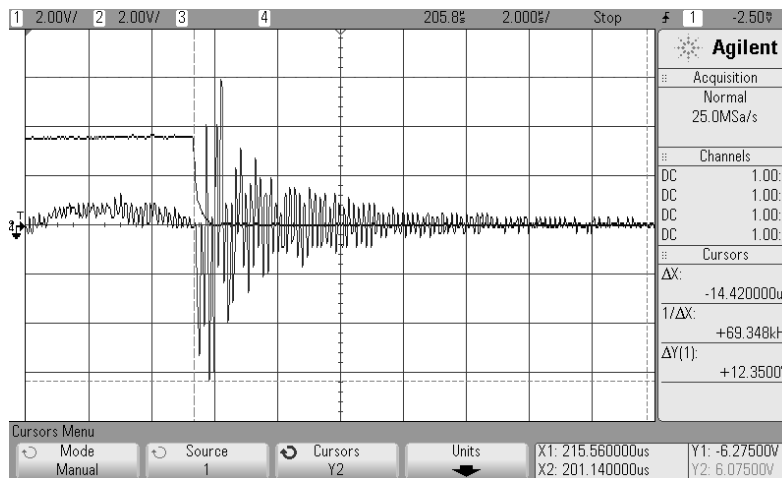


Figure 11. Decaying pulse signal.

Currently measurements have been made to see the number of peaks in the as prepared  $Ni_{1-x}Zn_xFe_2O_4$  sample which has a 25:75 sample to epoxy ratio, and  $x=0.2$ . This was compared the measurements also taken of sample Mu55-2 which is a powdered steel and is currently being used in the industry. The measurements were taken within frequency ranges of 0.1-1.2MHz with intervals of 0.02MHz. All possible resonant peaks were identified and then each were measured again as the pulse frequency to ensure they were real resonances. Some peaks turned out to be just noise, others were found to possibly be peaks but needed further testing. True resonant frequencies decayed exponentially slower. Frequency spectrum with their time domain signals are shown in figures 14-16 showing true resonances, noise and possible resonances respectively.

DEC15-17  
IMPROVED MAGNETIC SENSOR FOR OIL AND NATURAL GAS WELL LOGGING

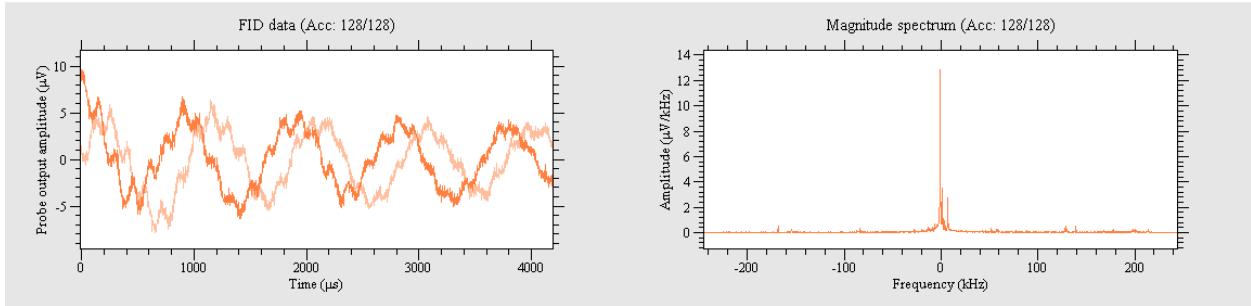


Figure 12. Sample Mu55-2 0.9 MHz.

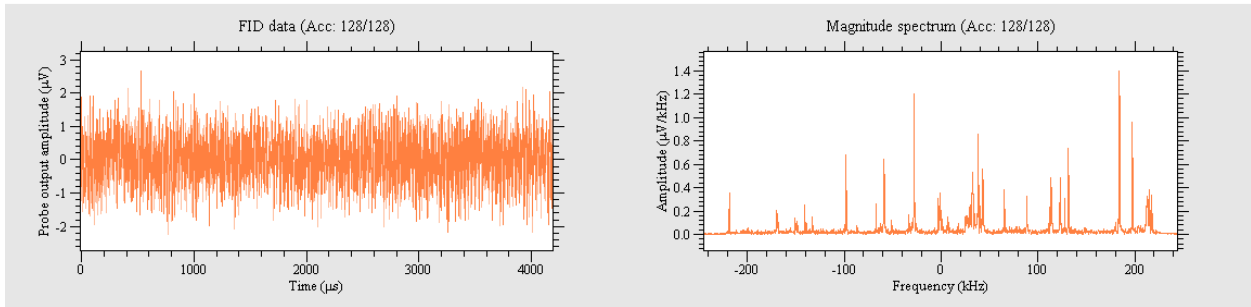


Figure 13. Sample Mu55-2 0.396 MHz.

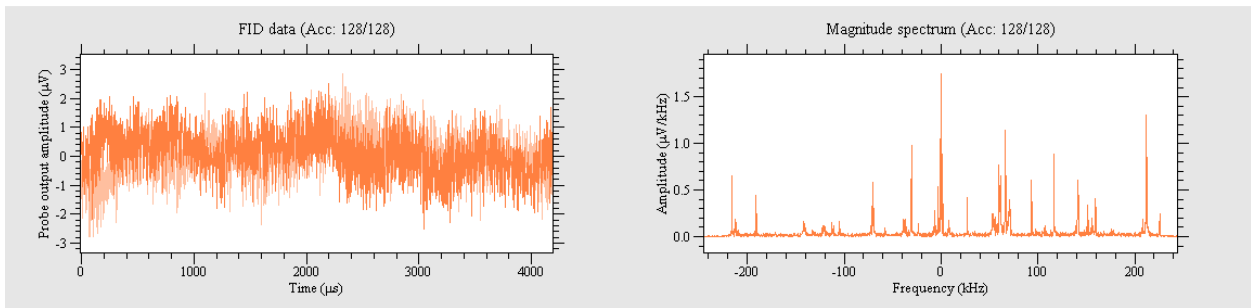


Figure 14. Sample Mu55-2 0.424 MHz.

Once the data is gathered for all probable peaks, the data is analyzed to find out if it actual a peak. The spectral bandwidth of the peak is found to determine the how fast the signal decays. From the time bandwidth law, there is a reciprocity between damping and spectral bandwidth. Hence, a larger spectral bandwidth means the time signal decays quickly and is more likely to have many non-zero components in the spectrum. Ideally, an undamped pulsed sinusoid like the RF signal being sent should have only a small spectral bandwidth if it is at the resonant frequency.

Currently, we are experimenting with a measurement setup that encloses the sample holder inside an Aluminum box as shown in figure 15. The number of turns in the inductor is 28.

DEC15-17  
IMPROVED MAGNETIC SENSOR FOR OIL AND NATURAL GAS WELL LOGGING

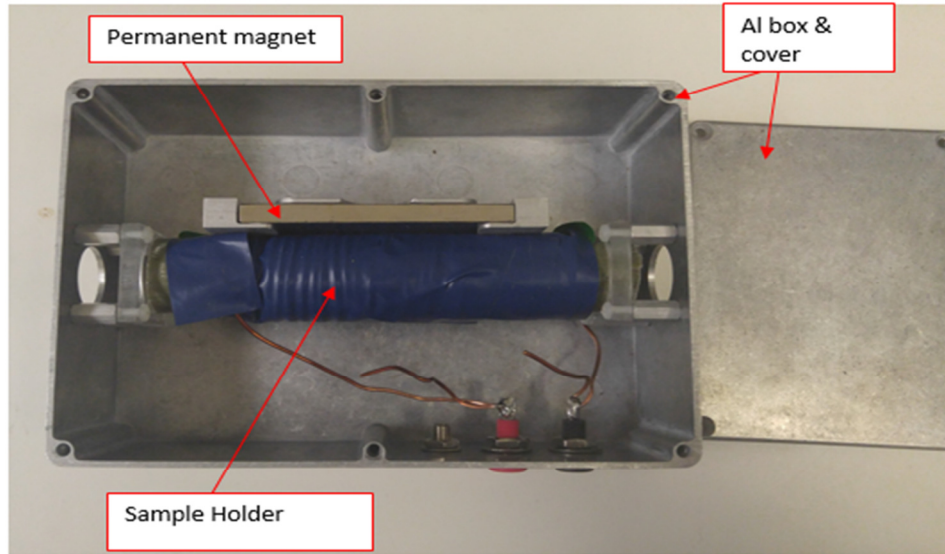


Figure 15. Assembled new sample holder with the increased magnetic field without top cover.

The samples that have been tested so far are the SA70, Ferrite epoxy made in Ames lab, and PI55. Only the resonances of the SA70 and Ferrite epoxy were confirmed with the box. A comparison was performed on the Ferrite epoxy measurements with or without the box. More peaks are seen with the box. The results are shown in the figures below.

ISU Ferrite without shielding possible resonances (30 turns)

Repetition time 7 s, scans 128, pulse acquisition delay 200 us, pulse amplitude 8 dB.

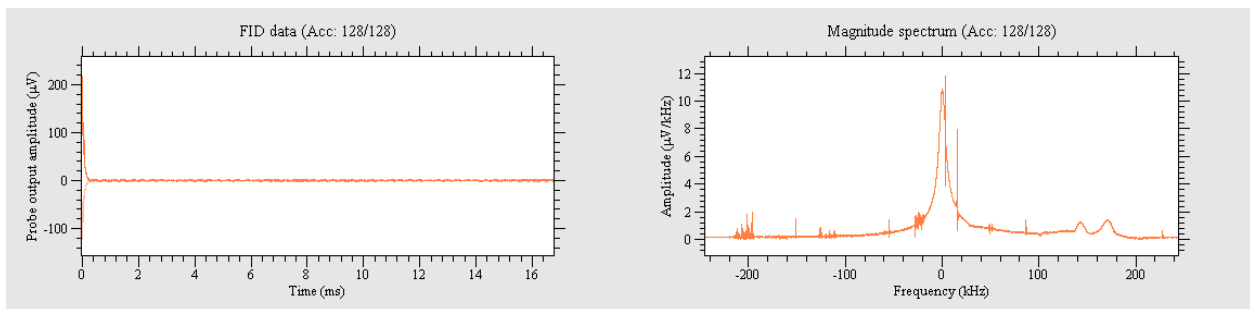


Figure 16. Center frequency 156.9 kHz.

DEC15-17  
IMPROVED MAGNETIC SENSOR FOR OIL AND NATURAL GAS WELL LOGGING

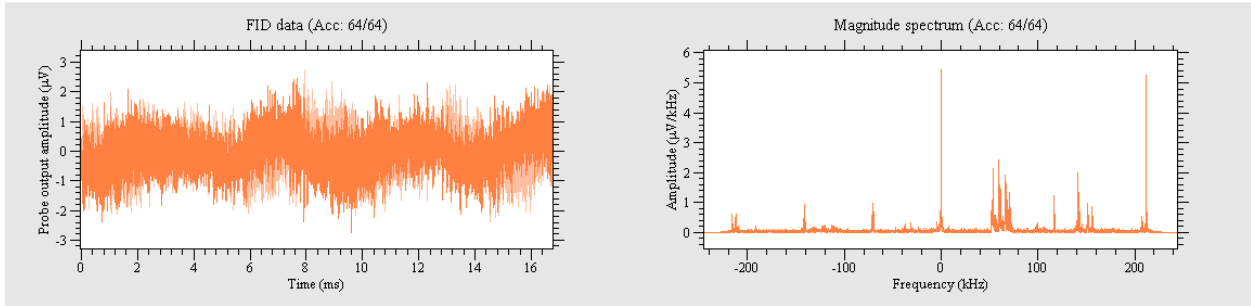


Figure 17. Center frequency 424 kHz.

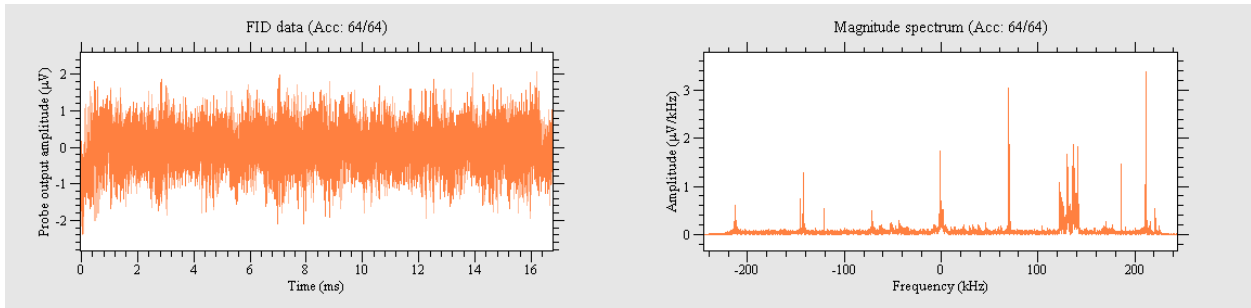


Figure 18. Center frequency 494 kHz.

MU701 with shielding resonances (28 turns)

Repetition time 7 s, scans 128, pulse acquisition delay 200 us, pulse amplitude 8 dB.

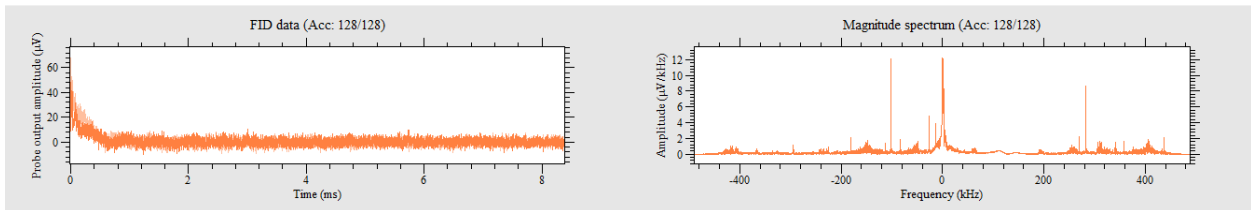


Figure 19. Center frequency 128.2 kHz.

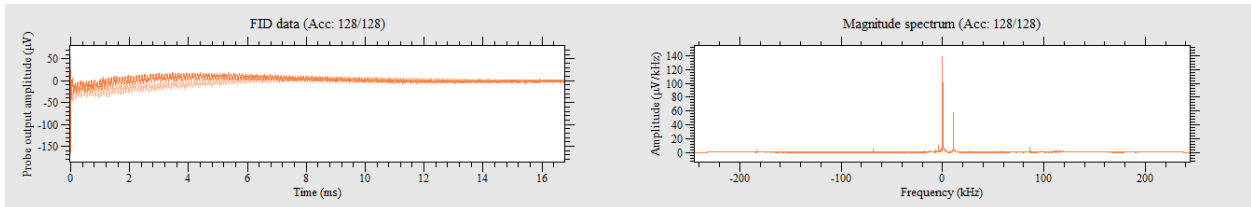


Figure 20. Center frequency 240 kHz.

DEC15-17  
IMPROVED MAGNETIC SENSOR FOR OIL AND NATURAL GAS WELL LOGGING

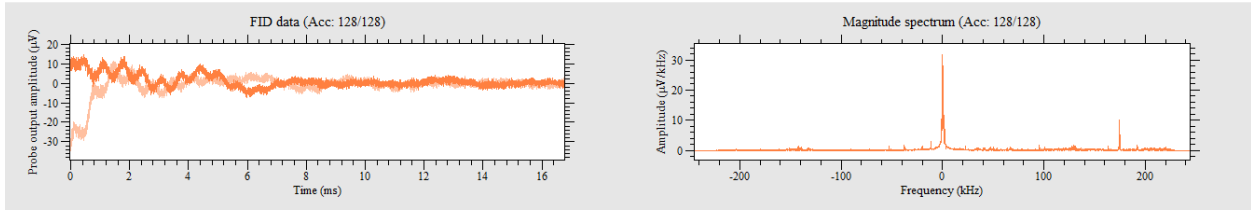


Figure 21. Center frequency 404 kHz.

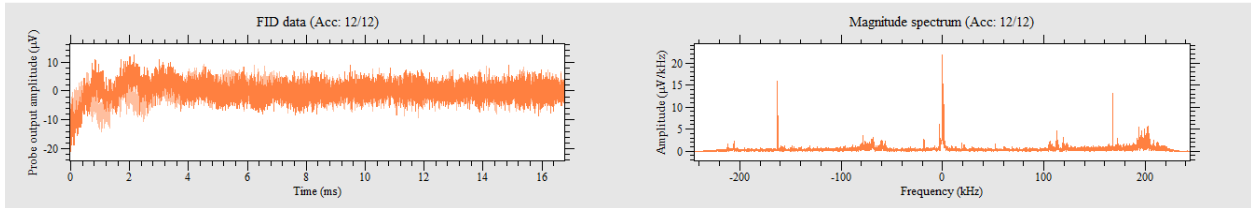


Figure 22. Center frequency 476.4 kHz.

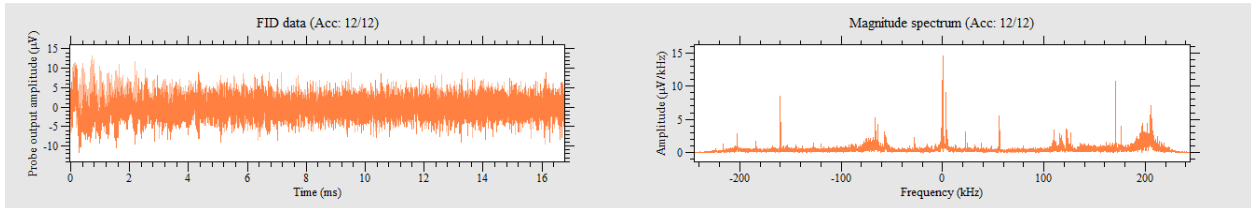


Figure 23. Center frequency 479.8 kHz.

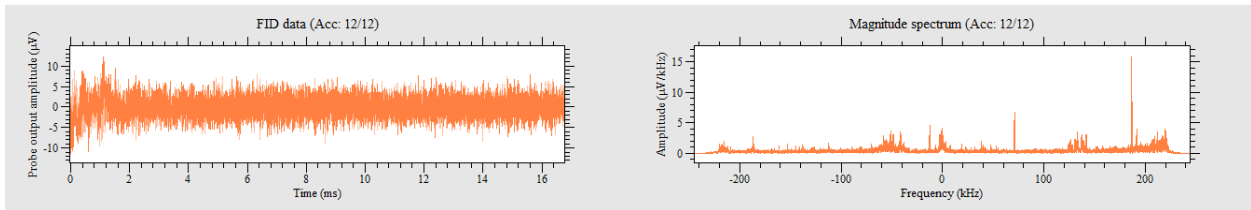


Figure 24. Center frequency 495 kHz.

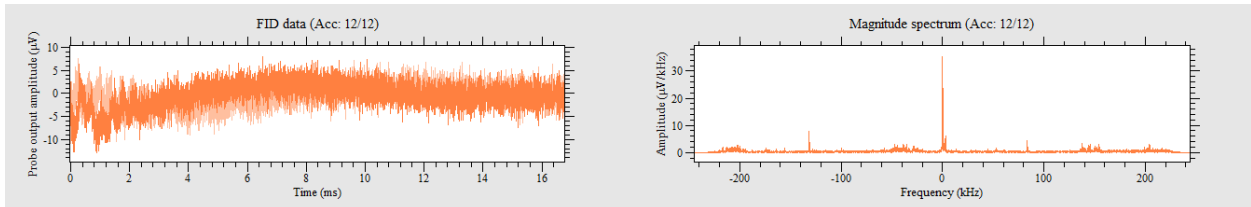


Figure 25. Center frequency 507.8 kHz.

DEC15-17  
IMPROVED MAGNETIC SENSOR FOR OIL AND NATURAL GAS WELL LOGGING

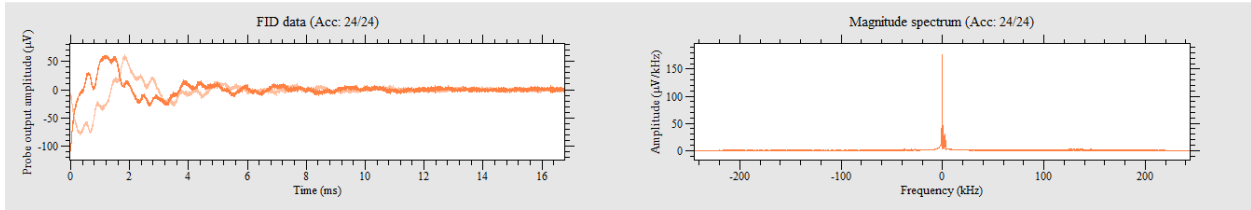


Figure 26. Center frequency 682 kHz.

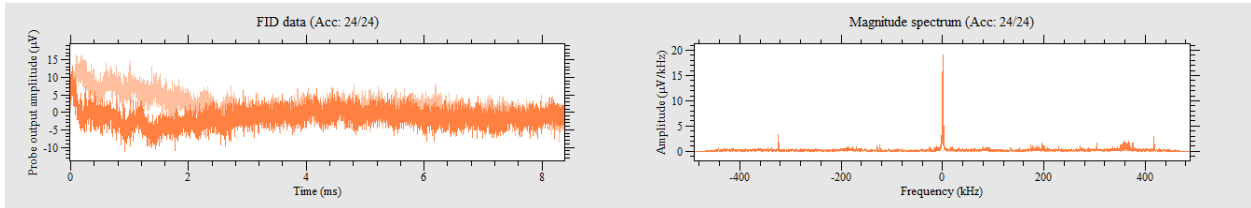


Figure 27. Center frequency 911.2 kHz.

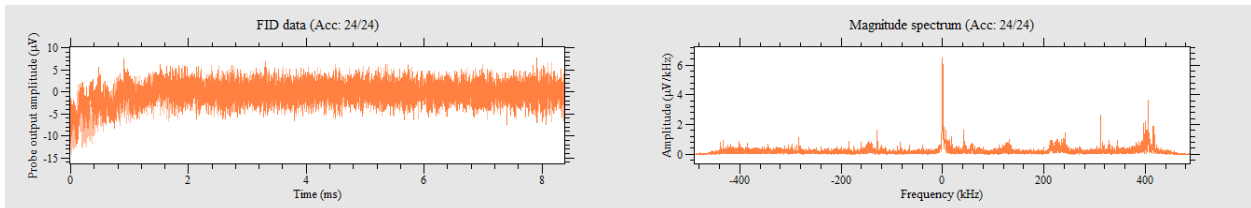


Figure 28. Center frequency 951.6 kHz.

ISU Ferrite with shielding resonances (28 turns)

Repetition time 7 s, scans 128, pulse acquisition delay 200 us, pulse amplitude 10 dB.

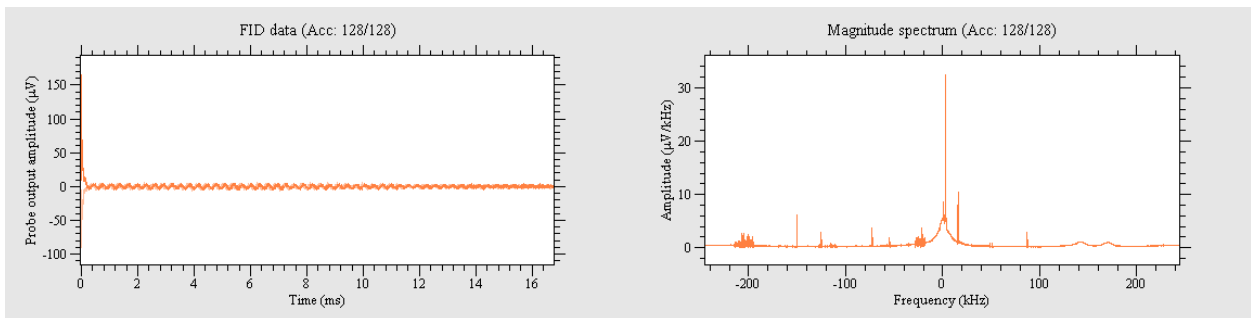


Figure 29. Center frequency 156.9 kHz.

DEC15-17  
IMPROVED MAGNETIC SENSOR FOR OIL AND NATURAL GAS WELL LOGGING

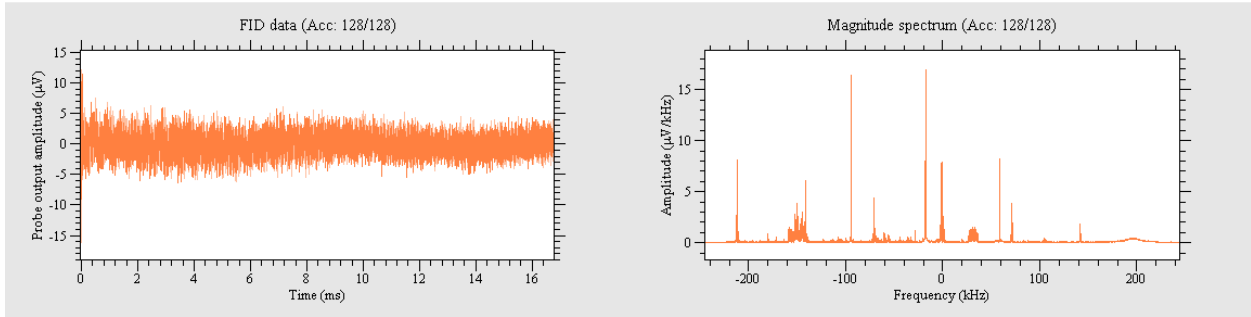


Figure 30. Center frequency is 212 kHz.

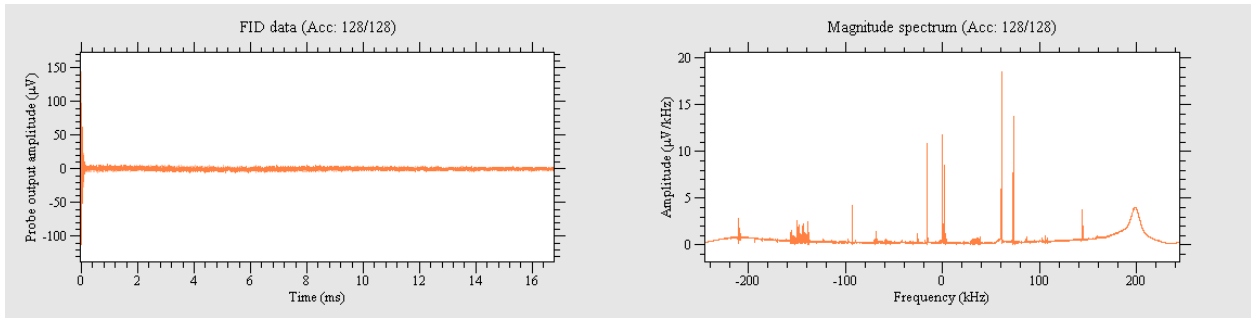


Figure 31. Center frequency 214 kHz.

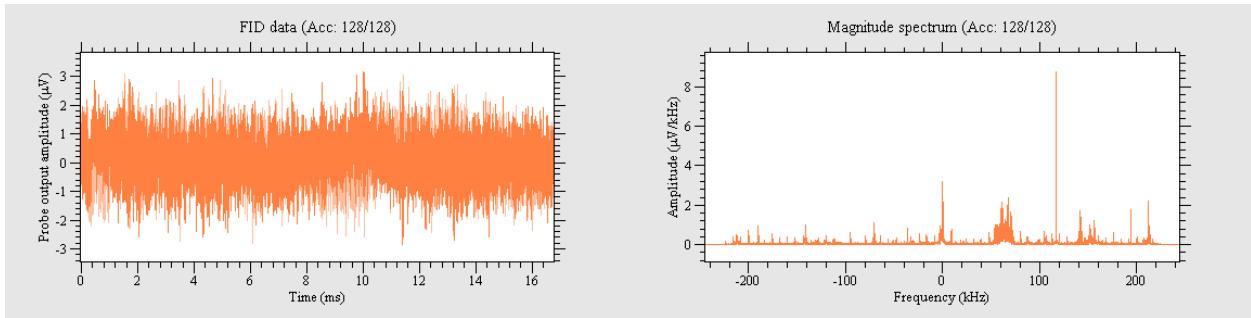


Figure 32. Center frequency 424.2 kHz.

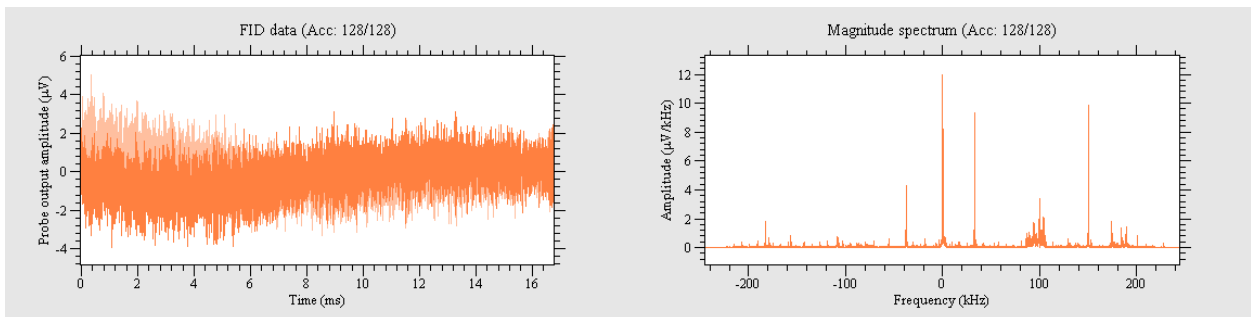


Figure 33. Center frequency 457 kHz.

DEC15-17  
IMPROVED MAGNETIC SENSOR FOR OIL AND NATURAL GAS WELL LOGGING

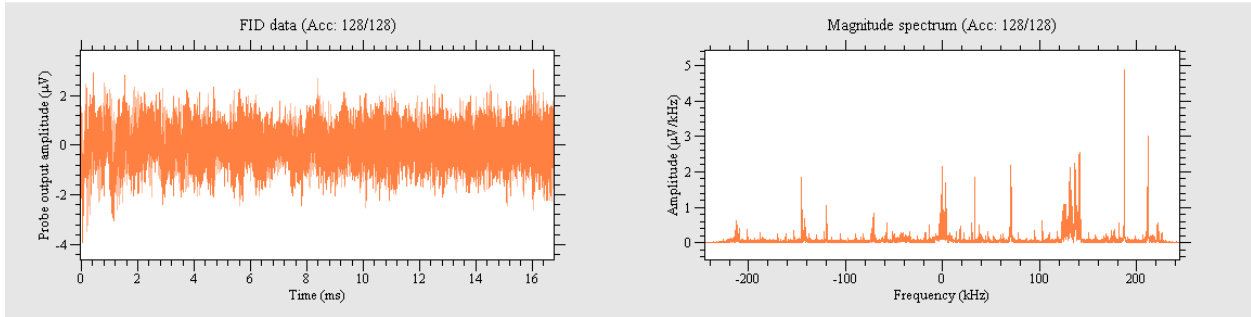


Figure 34. Center frequency 494.8 kHz.

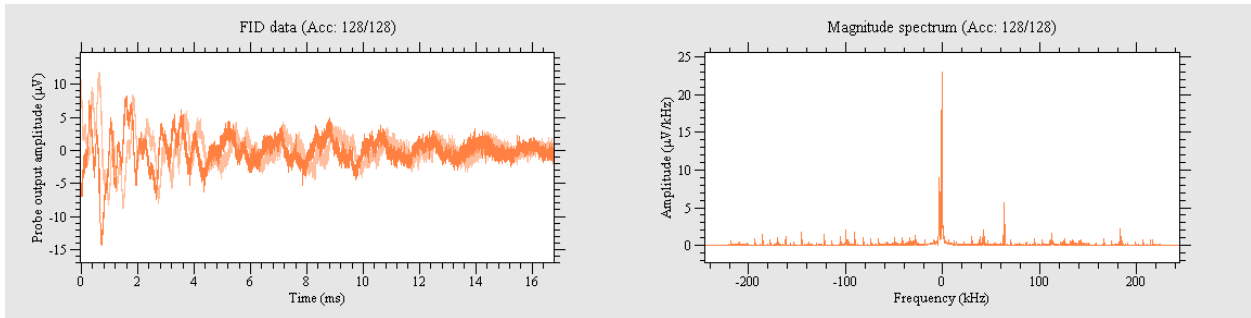


Figure 35. Center frequency 678.5 kHz.

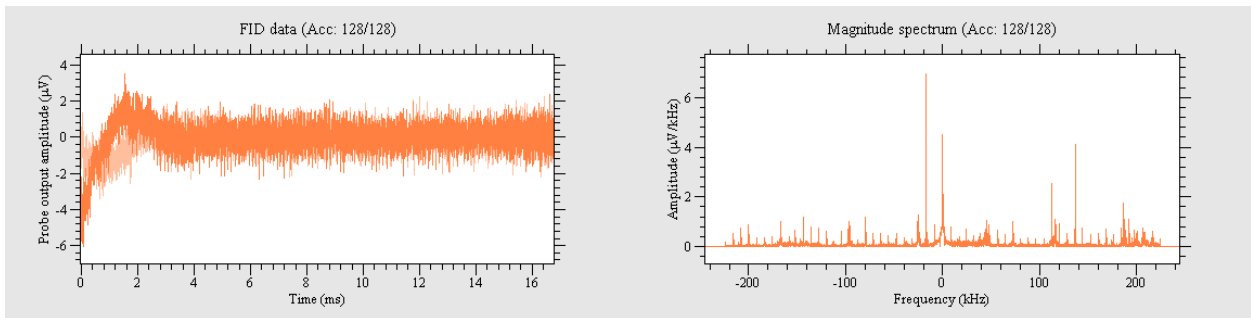


Figure 36. Center frequency 752 kHz.



DEC15-17  
IMPROVED MAGNETIC SENSOR FOR OIL AND NATURAL GAS WELL LOGGING

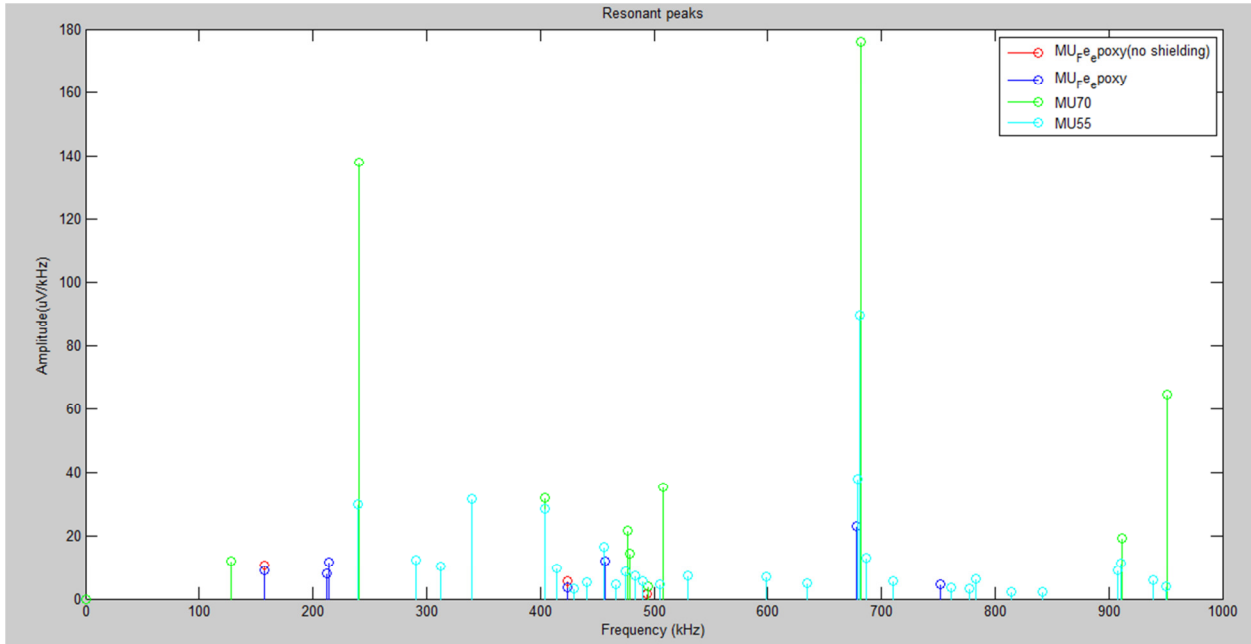


Figure 37. Comparison of MU70, MU55 and Ferrite epoxy peaks.

Out of all the measurements results, the MU55 fared the worst and the ISU Ferrite had the least amount of unwanted acoustics.

### Anomalous resonant frequencies

There were two anomalous resonant frequencies which were unusually strong in the 229 k and 1.135 k vicinity. They showed up for all samples tested. We currently have no explanation of what is causing them nor can we confirm that they are not resonant peaks from the sample. Even with an increased magnetic field as shown in figures 27 and 28, they are still very strong.

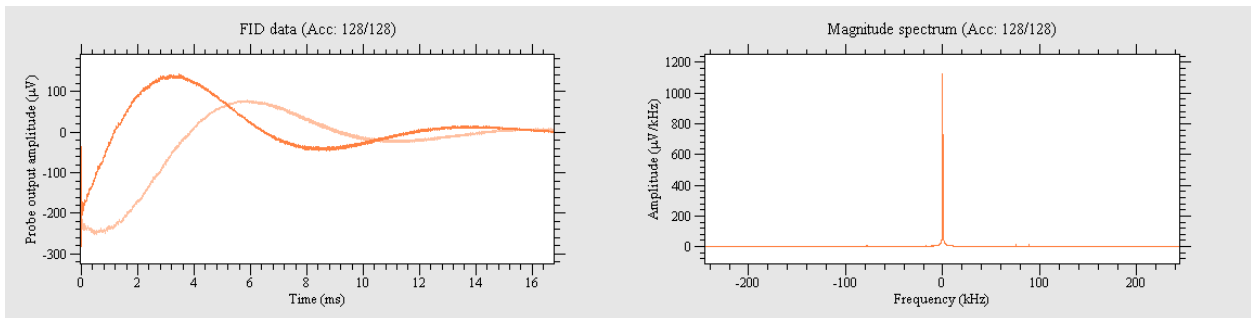


Figure 38. Anomalous peak center frequency 229 kHz for MU70 (increased magnetic field).

DEC15-17  
IMPROVED MAGNETIC SENSOR FOR OIL AND NATURAL GAS WELL LOGGING

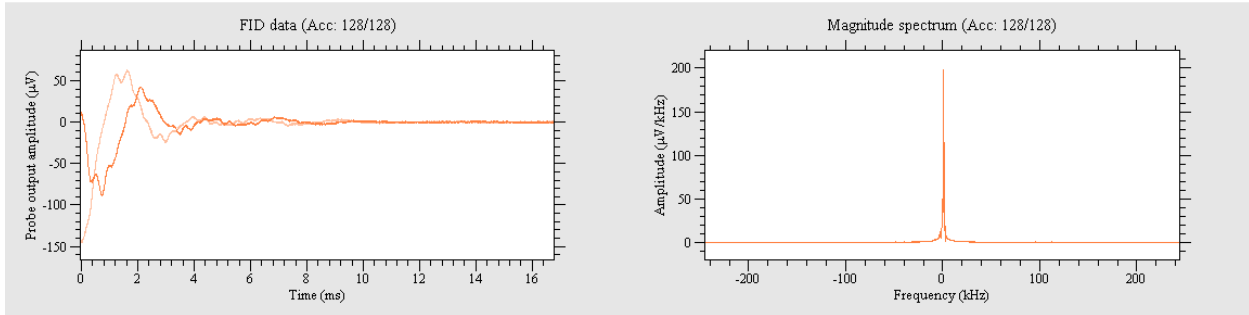


Figure 39. Anomalous peak center frequency 1.135 kHz MU70 (increased magnetic field).

Simulations are also being performed to find out if the unwanted resonances are actually coming from the circuit and the material. It takes into account the actual impedance coming out at the ends of the coil measured using an RLC meter. The ISU\_Ferrite sample was used for the simulation since it had the best measurement results. The circuit simulation is shown in figure below.

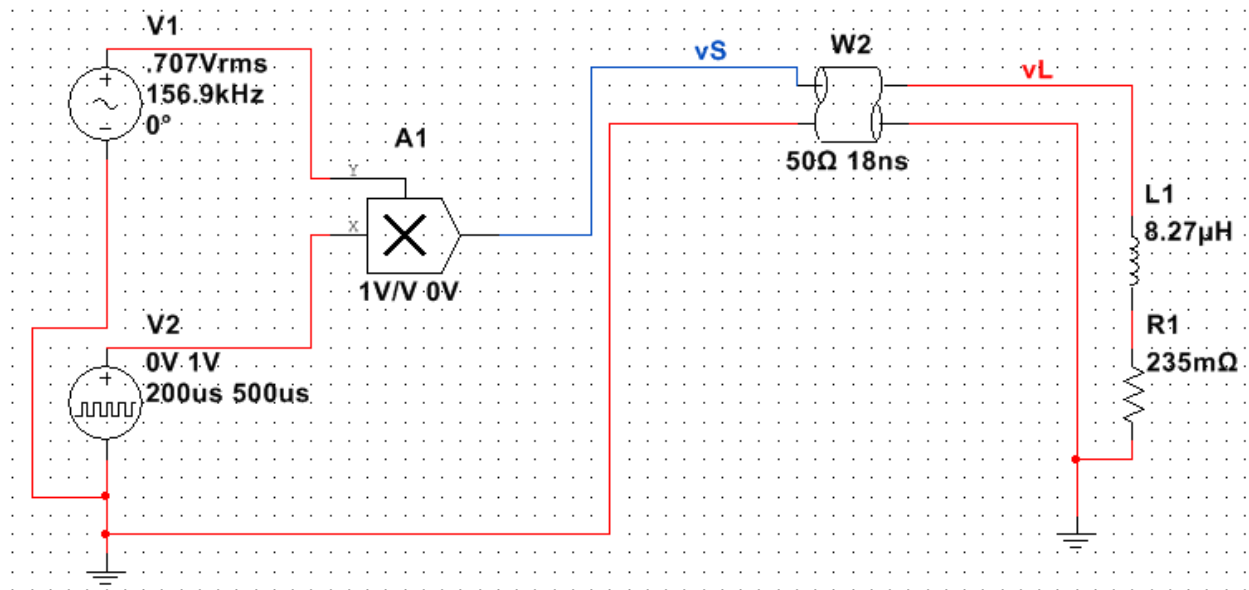


Figure 40. Circuit simulation schematic.

The time domain data shown in figure 41 shows that the load voltage doesn't simply die out once the pulse is turned off. There is still a residual signal left of a different frequency than the pulse. The load voltage is in red. The effect on reflections is much greater when the source voltage is off.

DEC15-17  
IMPROVED MAGNETIC SENSOR FOR OIL AND NATURAL GAS WELL LOGGING

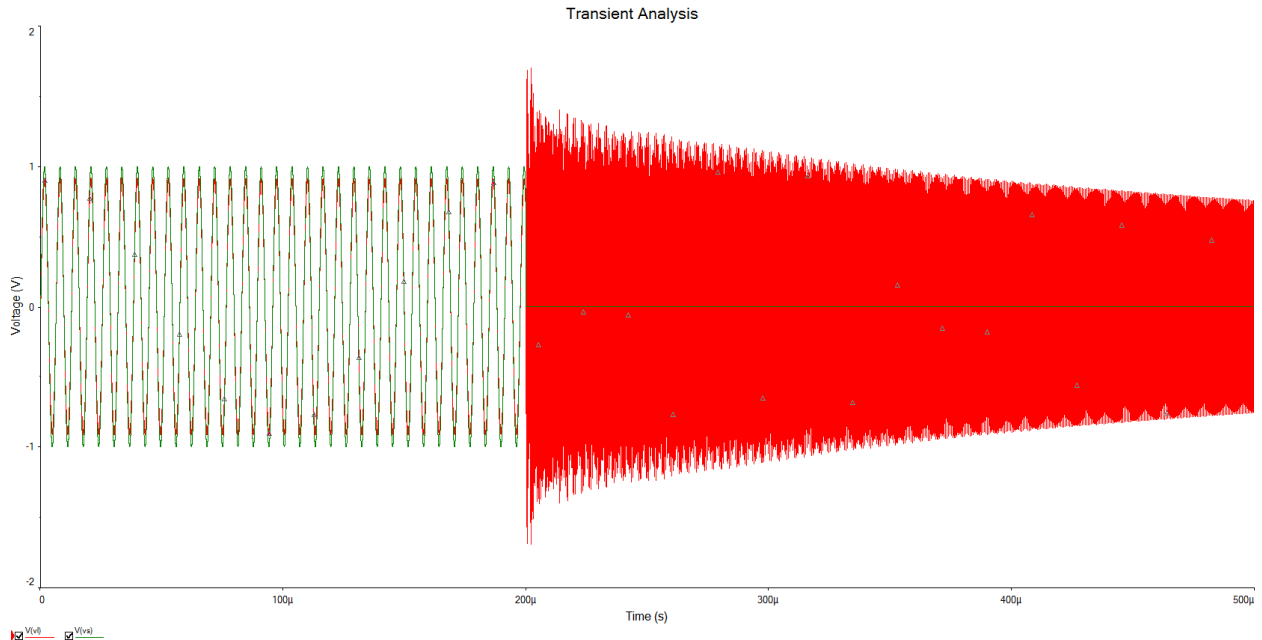


Figure 41. Transient analysis result center frequency 156.9 kHz.

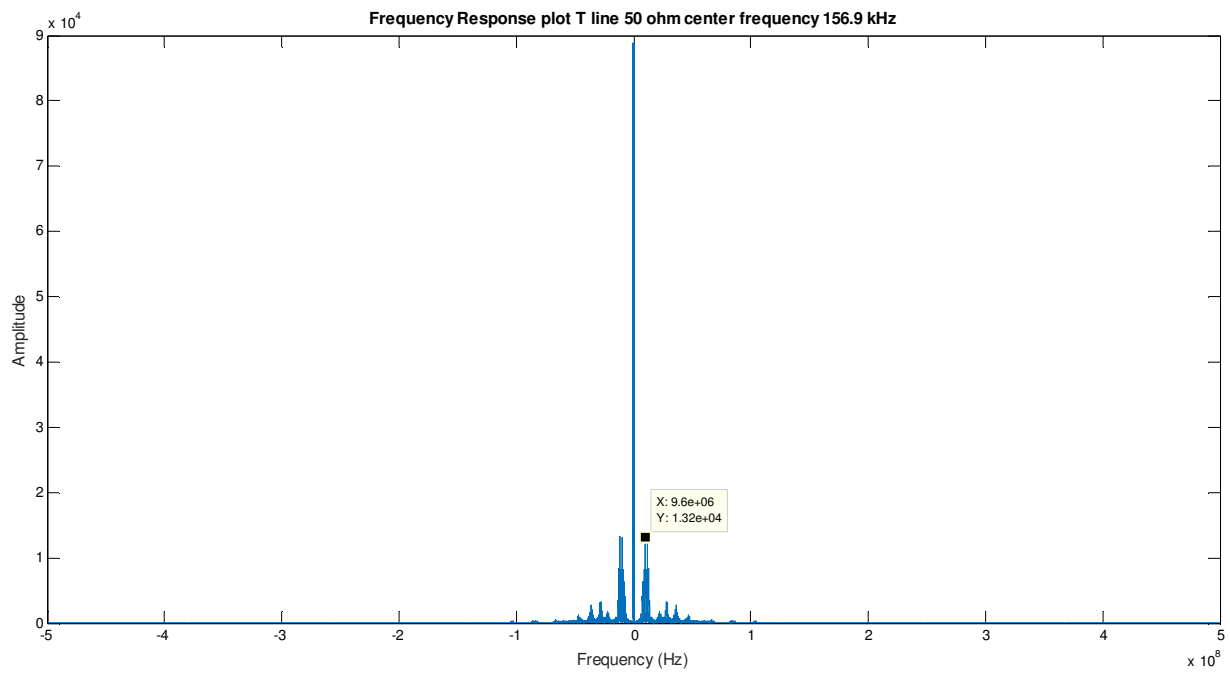


Figure 42. Frequency spectrum center frequency 156.9 kHz.

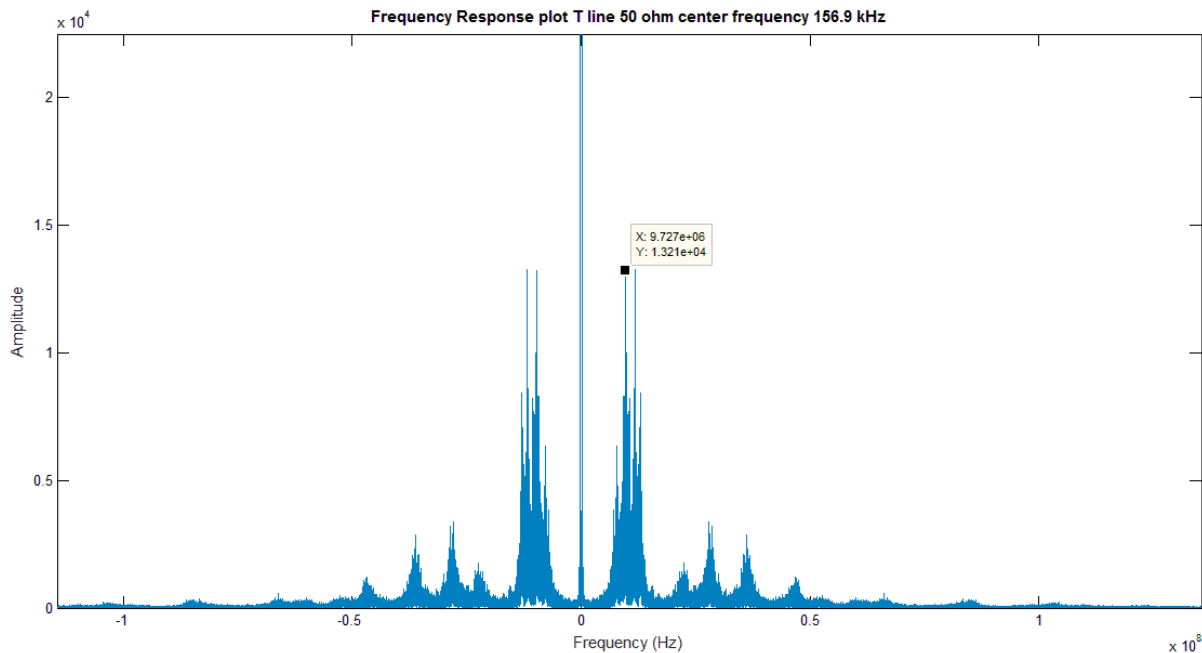


Figure 43. Zoom in of figure 42.

From the frequency domain data, we see that additional circuit resonance occur outside our range in this case they occur around 9 MHz. Our measurement range is around 0.1-1 MHz. So it is safe to suffice that they are not the cause of the unwanted acoustics. There is also a slight shift in the center frequency.

The future setup will be modified slightly to include the uniform field and the antenna will be rigged into it using a mechanical support system to dampen mechanical vibrations.

## Conclusion

The current design plan we have developed seeks to address the main issues with this project. The main issues in the project is unwanted resonances that appear in the NMR frequency spectrum and, the lack of uniform static magnetic field during testing. Our literature search has shown/revealed that using proper sample preparations methods such as annealing, in the right atmosphere and temperature, the soft magnetic properties can be improved. This can help reduce hysteresis losses in the magnetic core. Simulations in COMSOL show that using permanent magnets to create uniform static magnetic fields are possible and affordable. Our design plan therefore should be able to address the ringing problems in the sensor.

## References

- [1] P. Mathur et al., J. of Magn. Magn. Mater. 320 (2008) 1364–1369
- [2] P.Hu et.al, J. of Magn. Magn. Mater. 322 (2010) 173–177
- [3] K&J Magnetics: Neodymium Ring Magnets. N.p., n.d. Web. 31 Mar. 2015.
- [4] K&J Magnetics: Magnetics Blog. N.p., n.d. Web. 31 Mar. 2015.